THE EFFECTS OF METFORMIN ON OBESITY-INDUCED DIABETIC RETINAS

A Thesis

by

JEESU KIM

Submitted to the Office of Graduate and Professional Studies of
Texas A&M University
in partial fulfillment of the requirements for the degree of

MASTER OF SCIENCE

Chair of Committee,	Gladys Ko
Committee Members,	Louise Abbott
	Chaodong Wu
Head of Department,	Jane Welsh

August 2017

Major Subject: Biomedical Sciences

Copyright 2017 Jeesu Kim

ABSTRACT

Diabetic retinopathy is a major secondary complication of type 2 diabetes. To regulate blood glucose levels in type 2 diabetic patients, metformin is popularly prescribed as an oral drug in mono- and combination therapies. Metformin was used as a responsive and preventative drug on high-fat diet (HFD) induced obese mice that emulate type 2 diabetes. Body weight was monitored weekly and systemic glucose levels including resting blood glucose levels, the glucose tolerance test, and the insulin resistance test were measured monthly. The electroretinogram (ERG) was used to measure the retinal light responses, immunohistochemistry to quantify changes in retinal protein expression, western blot to assess inflammatory markers, and fluorescein angiography to measure neovascularization.

HFD-fed mice became hyperglycemic after 2 months of feeding regimen. Metformin treatment following hyperglycemia slowed body weight gain and restored systemic glucose levels to control levels. Retinal function measured by ERG showed decreased amplitudes and delayed implicit times in oscillatory potentials after 1 month of HFD and decreased amplitudes and delayed implicit times in a-wave, b-wave, and oscillatory potentials starting 2 months of HFD. Metformin treatment after 2 months of HFD was not able to restore ERG responses in HFD-fed mice. Furthermore, metformin treatment was not able to recover HFD-induced neovascularization. However, metformin treatment for the last 4 months in mice fed a HFD for 6 months was able to reduce inflammatory marker expression and the immunofluorescent proteins affected by HFD-

feeding. HFD-fed mice treated with metformin from the beginning of feeding regimen as a preventative strategy not only showed slower weight gain but also do not become hyperglycemic. However, this preventative strategy did not prevent the HFD-induced retinal dysfunction measured by ERG even after 3 months of treatment. Furthermore, some HFD-induced changes in retinal protein expression began after 1 month of HFD-treatment, but metformin treatment concurrent with HFD was not able to prevent HFD-induced changes.

CONTRIBUTORS AND FUNDING SOURCES

Contributors

This work was supervised by a thesis committee consisting of Associate Professor Gladys Ko of the Department of Veterinary Integrative Biosciences [advisor], Professor Louise Abbott of the Department of Veterinary Integrative Biosciences, Associate Professor Chaodong Wu of the Department of Nutrition and Food Science, and Professor Evelyn Tiffany-Castiglioni of the Department of Veterinary Integrative Biosciences.

Dr. Liheng Shi and Janet Chang assisted in handling mice. Kathryn Klotz assisted with technical data collection. All other work for the thesis was completed independently by the student.

Funding Sources

Graduate study was supported by a teaching assistantship from the Department of Veterinary Integrative Biosciences. This work was made possible in part by the U.S. National Institute of Health/National Eye Institute Grant NIHR21EY023339 to Dr. Gladys Ko.

TABLE OF CONTENTS

Page

CHAPTER I

INTRODUCTION*

Diabetic retinopathy (DR) is one of the major secondary complications of diabetes and a leading cause of blindness worldwide. [1] Glycemic control is a critical strategy for diabetic patients to prevent the development of secondary complications [2]. The Diabetes Control and Complications Trial showed that long-term extensive control of blood glucose reduces the incidence and progression of diabetic complications such as retinopathy, nephropathy, and neuropathy. [3] One drug that effectively controls systemic glycemia is metformin. [4, 5] Metformin has been used as an anti-hyperglycemic agent in diabetic patients, [6] and it is recommended in combination therapies to control the level of glycated hemoglobin (HbA1c) in patients with ineffective monotherapy, [7] The effectiveness of metformin as an anti-hyperglycemic agent is based on its ability to suppress gluconeogenesis in the liver. [5, 8] In addition to its use as an anti-hyperglycemic agent, one beneficial effect from metformin is mild weight loss. [9-11] The action of metformin on insulin signaling has made metformin viable for treating non-alcoholic fatty liver disease [12] and polycystic ovary syndrome. [13] Furthermore, the effectiveness of metformin to treat other diabetic complications, such as nephropathy [14] and neuropathy has been investigated. [15] However, whether metformin is able to prevent or reverse DR is not known.

---

*Reprinted with permission from Kim AJ, Chang JY-A, Shi L, Chang RC-A, Ko ML, Ko GY-P. The effects of metformin on obesity-induced dysfunctional retinas. *Invest Ophthalmol Vis Sci*. 2017;58:106-118. Copyright 2017 Association for Research in Vision and Ophthalmology

In the US, obesity associated type 2 diabetes has reached epidemic proportions with more than 68% of American adults considered overweight or obese (http://win.niddk.nih.gov/statistics/index.htm). More than 60% of type 2 diabetic patients will develop DR. [16, 17] The high-fat-diet (HFD) mouse model is used to study type 2 diabetes due to the development of obesity, glucose intolerance, and insulin resistance. [18] Unlike other mouse models of metabolic syndromes and type 2 diabetes that utilize genetic mutations to induce insulin resistance and obesity, [19] the HFD model is a diet-induced obesity model that resembles human obesity-associated type 2 diabetes. The HFD mice develop hyperglycemia, hyperinsulinemia, hyperlipidemia, and chronic inflammation after several months of HFD regimen and are suitable to study long-term diabetic complications. [20, 21] These HFD mice show similar phenotypical deficits found in other DR animal models, such as lesions in the retinal vasculature and thickening of Bruch's membrane. [22] Furthermore, mice fed with a HFD containing 42% fat calories for 12 months have significantly greater numbers of atrophic capillaries and pericyte ghosts compared to mice fed with a normal diet. [23] HFD mice emulate the systematic dysfunction that occurs in type 2 diabetes and further show retinal symptoms found in DR, thus making HFD-mice a suitable animal model to study type 2 diabetes and diabetic retinopathy.

Previously, we reported that mice fed with a HFD (59% fat calories) develop obesity, hyperglycemia, insulin resistance, glucose intolerance, and decreased retinal light sensitives. [24] These mice have retinal neovascularization after 7 months of HFD regimen. [25] Since metformin is able to maintain normal systemic glycemia in diabetic

animals and patients, [4, 5] in this study, we examined whether metformin was able to reverse or minimize HFD-induced retinal dysfunction. We combined electroretinogram (ERG) recordings, immunofluorescent staining, fluorescein angiography (FA), and western blotting to determine the effects of metformin in HFD-induced diabetic retina. Furthermore, metformin has been studied in clinical trials to prevent the incidence of type 2 diabetes in individuals who are prediabetic. [26, 27] Therefore, we examined whether concurrent treatment of metformin before hyperglycemia was able to prevent the development of HFD-induced retinal dysfunction and changes in retinal protein expression through means of ERG recordings and immunofluorescent staining, respectively.

CHAPTER II

MATERIALS AND METHODS*

Animals

Four week old male C57BL/6J mice were purchased from Harlan (Houston, TX, USA) and the Jackson Laboratory (Bar Harbor, Maine, USA). All animal experiments were approved by the Institutional Animal Care and Use Committee of Texas A&M University (AUP# 2014-0285) and were performed in compliance with the ARVO Statement for the Use of Animals in Ophthalmic and Vision Research. Mice were housed under temperature and humidity-controlled conditions with 12:12 hour light–dark cycles. All mice were given food and water *ad libitum.* At 5 weeks of age (body weight at 20 g), mice were fed with a standard laboratory chow (control; 10% fat calories, 20% protein calories, and 70% carbohydrate calories; Research Diets, Inc., New Brunswick, NJ, USA) or a high fat diet (HFD; 59.4% fat calories, 18.1% protein calories, and 22.5% carbohydrate calories; TestDiet®, St. Louis, MO, USA). After 2 months of HFD regimen, some HFD-mice were given daily metformin treatments at a dosage of 150 mg/Kg through oral gavage as the HFD+Met group. Some HFD mice were given daily oral gavage of metformin at 200 mg/kg concurrently from the beginning of the feeding regimen as the HFD+Pre-met group. Body weight and food intake were measured weekly. Non-fasting blood glucose levels, glucose tolerance, and

*Reprinted with permission from Kim AJ, Chang JY-A, Shi L, Chang RC-A, Ko ML, Ko GY-P. The effects of metformin on obesity-induced dysfunctional retinas. *Invest Ophthalmol Vis Sci*. 2017;58:106-118. Copyright 2017 Association for Research in Vision and Ophthalmology

insulin resistance were measured monthly by taking blood from the tail vein. Glucose levels were measured using the Clarity Plus Blood Glucose Monitoring System (Diagnostic Test Group, Boca Raton, FL, USA).

Glucose tolerance and insulin resistance tests

Mice were fasted for 8 hours and given a single intraperitoneal (i.p.) injection of D-glucose (Sigma-Aldrich, St. Louis, MO, USA) at a dosage of 2 g per kg body weight for the glucose tolerance test or insulin (Gibco/Life Technologies, Grand Island, NY, USA) at a dosage of 1 unit per kg body weight for the insulin resistance test. Blood glucose levels were measured from the tail vein using the Clarity Plus Blood Glucose Monitoring System (Diagnostic Test Group) at 0, 30, 60, 90, and 120 minutes following the glucose injection during the glucose tolerance test. Blood glucose levels were measured at 0, 15, 30, 45, and 60 minutes following the insulin injection during the insulin resistance test.

***In vivo* electroretinogram**

The *in vivo* electroretinogram (ERG) recordings of retinal light responses were performed as described previously. [24] Mice were dark adapted for a minimum of 3 hours and anesthetized with an i.p. injection of Avertin (2% 2,2,2-tribromoethanol, 1.25% *tert*-amyl alcohol; Fisher Scientific, Pittsburgh, PA, USA) solution (12.5 mg/ml) at a dosage of 500 µl per 25 g body weight. Pupils were dilated using a single drop of 1% tropicamide / 2.5% phenylephrine mixture for 5 minutes. Mice were placed on a heating

pad to maintain body temperature at 37°C. The ground electrode was placed on the tail and the reference electrode placed under the skin in the cheek below the eye. A thin drop of Goniovisc (Hub Pharmaceuticals, Rancho Cucamonga, CA, USA) was applied on the surface of the cornea to keep it moist, and a threaded recording electrode conjugated to a mini contact lens (Ocuscience, Henderson, NV, USA) was placed on top of the cornea. All preparatory procedures were done under dim red light, and the light was turned off during the recording. A portable ERG device (OcuScience) was used to measure scotopic ERG recordings at light intensities of 0.1, 0.3, 1, 3, 10, and 25 cd·s/m^2. Responses to four light flashes were averaged at the lower light intensities (0.1, 0.3, 1.0, and 3.0 cd·s/m^2) while only one light flash was applied for the higher light intensities (10 and 25 cd·s/m^2). A one minute recovery period was programmed between different light intensities. The amplitudes and implicit times of the a-wave, b-wave, and oscillatory potentials (OPs) were recorded and analyzed using the ERGView 4.4 software (OcuScience). Both eyes were included in the analyses and their values were averaged.

Immunofluorescent staining

Mice were put under deep anesthesia through isoflurane (Zoetis, Parsippany, NJ, USA) and cervical dislocation was performed. Mouse eyes were excised and prepared as previously described. [24] In brief, eyes were fixed with Zamboni fixative and processed for paraffin sectioning at 4 µm. Each glass slide contained single paraffin sections from the control and experimental groups. After deparaffinization and antigen retrieval,

sections were washed in PBS, blocked with 10% goat serum for 2 hours at room temperature, and then incubated overnight with primary antibodies at 4 °C. The next day, sections were washed with PBS several times and incubated with fluorescent conjugated secondary antibodies for 2 hours at room temperature and mounted with ProLong Gold antifade reagent containing 4',6-diamidino-2-phenylindole (DAPI; Invitrogen/Life Technologies, Grand Island, NY, USA). The primary antibodies used were anti-phospho-protein kinase B ($pAKT_{Thr308}$; 1:100; Cell Signaling Technology, Danvers, MA, USA), anti-AKT (total AKT, 1:100; Cell Signaling Technology), anti-di-phospho-extracellular signal-regulated kinase (pERK, 1:100 Sigma-Aldrich, St. Louis, MO, USA), anti-ERK (total ERK, 1:100, Santa Cruz Biochemicals, Dallas, TX, USA), anti-phospho-AMPK ($pAMPK_{Thr172}$, 1:100, Cell Signaling Technology), anti-AMPK (total AMPK, 1:100, Cell Signaling Technology), anti-phosphorylated NF-κB (nuclear factor κ-light-chain enhancer of activated B cells complex) P65 at Ser536 (pP65; Cell Signaling Technology), NF-κB P65 (Total P65; Cell Signaling Technology, 1:100, Cell Signaling Technology), anti-$Ca_v1.3$α1D (L-type voltage gated calcium channel α1D subunit, 1:100, Chemicon International, Temecula, CA, USA). The secondary antibodies used were Alexa Fluor 488 goat anti-rabbit IgG (1:150; Molecular Probes/Life Technologies, Grand Island, NY, USA) and Cy5 goat anti-mouse IgG (1:150; Abcam, Cambridge, MA, USA). The images were taken under a Zeiss Stallion microscope (Carl Zeiss AG, Oberkochen, Germany). Each fluorescent image from the control and other experimental groups were taken under identical settings, including the same exposure time and magnification. Image analysis: In the control, HFD, and

HFD+Met group, 3 fluorescent images (n=3) after 7 months treatment were selected and analyzed from each retinal tissue section, which included all of retinal layers (from the photoreceptor outer segment to the ganglion cell layer). In the control, HFD, and HFD+Pre-met groups, 4 fluorescent images (n=1) after 1 month treatment were selected and quantified for the inner segments of the photoreceptors and also across all the retinal layers (from the outer segments of photoreceptors to the ganglion cell layer). The averaged fluorescent intensity per pixel for each image was quantified without any modification using the luminosity channel of the histogram function in the Adobe Photoshop 6.0 software (Adobe Systems, San Jose, CA, USA), and the green or red fluorescent intensities were measured on a scale of 0-255.

Fluorescein angiography

Mice were anesthetized with an i.p. injection of Avertin (12.5 mg/ml) at a dosage of 500 µl per 25 g body weight. Pupils were dilated using a single drop of 1% tropicamide / 2.5% phenylephrine mixture for 5 minutes. Immediately following pupil dilation, 10% sodium fluorescein (Akorn, Lake Forest, Illinois, USA) was i.p. injected at a dosage of 50 µl per 25 g body weight. Images were taken using the iVivo Funduscope for small animals (Ocuscience). The vascular parameters were further analyzed with Adobe Photoshop 6.0 (Adobe Systems) and the AngioTool software, a free software developed by the National Cancer Institute of National Institutes of Health (NCI/NIH, Bethesda, MD, USA) [28]. Square areas of 289 x 289 pixel^2 in the central retina (400 pixels from the optic nerve), as well as in the peripheral retinal region (800 pixels from

the optic nerve) were cropped with Adobe Photoshop. For each FA cropped image, at least 2 areas from the central and peripheral retinal regions were obtained to analyze the microvascular density (the percentage of vascular area to the retinal area), vessel area, vessel branch points, and the average non-vascular area (avg. lacunarity) using AngioTool. The primary retinal arteries and veins were not included in the analyses.

Western immunoblot analysis

Retina samples were collected as previously described. [24, 25] In brief, 2 retinas from a single mouse were pooled and counted as one sample. Intact retinas were homogenized in a Tris lysis buffer (50 mM Tris, 1 mM EGTA, 150 mM NaCl, 1% Triton X-100, 1% β-mercapto-ethanol, 50 mM NaF, 1 mM Na_3VO_4; pH = 7.5). Samples were separated on 10% sodium dodecyl sulfate-polyacrylamide gels by electrophoresis and transferred to nitrocellulose membranes. The primary antibodies used were anti-phosphorylated NF-κB (nuclear factor κ-light-chain enhancer of activated B cells complex) P65 at Ser536 (pP65; Cell Signaling Technology) and NF-κB P65 (Total P65; Cell Signaling Technology). Blots were visualized by using appropriate secondary antibodies conjugated to horseradish peroxidase (Cell Signaling Technology) and an enhanced chemiluminescence detection system (Pierce, Rockford, IL, USA).

Statistical analyses

All data are presented as mean ± standard error of mean (SEM). Statistical analyses were carried out using the Origin 8.6 software (OriginLab, Northampton, MA,

USA). Student's *t*-test was used for statistical analyses between the control and HFD group. One-way analysis of variance (ANOVA) followed by Tukey's *post hoc* test was used for statistical analyses between the control, HFD, and HFD+Met/ Pre-met groups. Throughout, the sample size "n" was the number of animals per group included in the analyses. $p < 0.05$ was regarded as significant.

CHAPTER III

RESULTS*

Metformin decelerated body weight gain and reversed hyperglycemia in HFD-induced diabetic animals

Mice fed with a HFD for 2 weeks (open circle) already had a significant weight gain compared to control mice (open square; Fig. 1A). Treatment with metformin in HFD-induced obese mice (gray triangle) significantly slowed down their weight gain compared to HFD-mice without metformin intervention (Fig. 1A). Mice under the HFD regimen for 2 months developed hyperglycemia (Fig. 1B), but after metformin treatment for only 1 month, the non-fasting blood glucose level of these HFD-mice returned to normal levels (Fig. 1B). The glucose tolerance test performed after 1 month of metformin treatment further verified the effectiveness of metformin in anti-hyperglycemia and reversing the glucose intolerance in HFD-obese mice back to the control level (Fig. 1C). Furthermore, the insulin resistance test performed after 1 month of metformin treatment also showed metformin's ability to recover insulin resistance in HFD-obese mice (Fig. 1D). Hence, metformin was effective in controlling systemic glycemia and weight gain.

---

*Reprinted with permission from Kim AJ, Chang JY-A, Shi L, Chang RC-A, Ko ML, Ko GY-P. The effects of metformin on obesity-induced dysfunctional retinas. *Invest Ophthalmol Vis Sci*. 2017;58:106-118. Copyright 2017 Association for Research in Vision and Ophthalmology

HFD-induced retinal dysfunction began with dampened oscillatory potential responses

We previously showed that retinal light responses decreased after mice were fed a HFD for 3 months. [24] To further determine when HFD-induced obesity caused retinal dysfunction, we measured the retinal light sensitivities with scotopic ERG recordings after the mice were fed with the HFD for only 1 month. We found that the amplitudes of ERG a- and b-waves were similar between the HFD-mice (gray circle) and the control (open square; Fig. 2A, 2B), but the HFD-mice had longer a- and b-wave implicit times (Fig. 2B). These HFD-mice also had significantly decreased OP amplitudes and delayed OP implicit times compared to the control mice (Fig. 2A, 2C), which indicates a possible early sign of obesity-induced retinal dysfunction, since a delayed OP latency is the first sign of an early diabetic retina in both rodents and humans. [29-31]

Metformin treatment did not improve the HFD-induced decreases in retinal light responses

After 2 months of HFD, the retinal light responses in HFD-mice (gray circle) were further deteriorated (Fig. 3). Compared to the control mice (open square), these HFD-mice had decreased a- and b-wave amplitudes (Fig. 3A and 3B) in addition to the functional deficits previously observed after 1 month of HFD (Fig. 3A and 3C). After 5 months of HFD, the retinal light responses in these HFD-mice (open circle) were worsen and significantly lower than the control mice (open square; Fig. 4). However, the retinal light responses in HFD-mice treated with metformin (HFD + Met; gray triangle) did not

improve as measured by ERG a- and b-waves (Fig. 4A and 4B), and their OPs were further aggravated (Fig. 4A and 4C), even though these HFD-mice had been treated with metformin for the last 3 months (Fig. 4D).

Metformin restored cell-signaling proteins in the retina that were affected by HFD

Although metformin did not recover HFD-induced retinal dysfunction, we next examined whether oral administration of metformin impacted the retina of HFD-mice at the molecular level. We determined the activation/phosphorylation of AKT, [32, 33,34,35, 36] ERK, [37] and AMPK [38] signaling, since these kinases are critical in cell metabolism, growth, and survival. Mice under HFD for 6 months (HFD) had a decrease in the phosphorylation of AKT (pAKT) and AMPK (pAMPK) but an increase in activated ERK (pERK) in the retina, and there was no apparent change in the total amount of AKT, ERK, and AMPK in the HFD-retina compared to control mice (Con; Fig. 5). The retinas from HFD-mice (under a HFD for 6 months) that were treated with metformin for 4 months (HFD+Met) had a recovery in these signaling molecules: pAKT was no longer dampened and similar to the control, pAMPK had increased compared to the control, and the level of pERK was decreased and comparable to the control level (Fig. 5). Interestingly, the retinas from these metformin-treated HFD-mice (HFD+Met) had an apparent up-regulation of total AMPK and pAMPK compared to control mice, which indicated that metformin might have a direct effect on AMPK in the neural retina, since metformin is known to up-regulate the expression and activation of AMPK in the kidney, [39] adipose tissue, [40, 41] and heart. [42]

Metformin treatment did not rescue HFD-induced neovascularization in the retina

We recently demonstrated that after 6 months of HFD, these HFD-mouse retinas develop neovascularization with an apparent increase of microaneuryism-like structures, [25] so we examined whether metformin treatments could stop the process of neovascularization in the HFD-mouse retina. We used FA and AngioTool [28] to compare changes in the central and peripheral retinal vasculature of the control, HFD, and HFD + Met mice (Fig. 6A). In the central retina, there were no differences in any vascular parameters between the three experimental groups (Fig. 6B). However, in the peripheral retina, mice under HFD for 6 months (HFD) had a significant increase in vascular density, vessel area, and the number of branch points compared to the control mice (Fig. 6C), while the average retinal area without detectable vasculature (avg. lacunarity) was decreased in HFD mice (HFD) and HFD-mice treated with metformin (Fig. 6C). Thus, mice under HFD for 6 months had retinal neovascularization, but treatment with metformin for 4 months (HFD+Met) did not improve HFD-caused retinal neovascularization (Fig. 6C). No differences in neovascularization in HFD-mice were observed at 5 months of feeding-regimen compared to control mice (data not shown).

Metformin treatment decreased inflammation

Since metformin has anti-inflammatory properties, [43] we determined if metformin could reverse HFD-induced retinal inflammation. Western blot analysis showed a significantly higher expression of phosphorylated P65 (pP65), a subunit of nuclear factor κ-light-chain-enhancer of activated B cells (NF-κB) transcription complex

and a biomarker for inflammation, [44] in HFD-mouse retina (HFD) compared to controls (Con), but the retina of HFD-mice treated with metformin (HFD+Met) had less pP65 compared to the HFD-mouse retina (Fig. 7A). These data provided evidence that metformin indeed reduced retinal inflammation in HFD-mice.

Treatment with metformin concurrently with the HFD regimen from the beginning delays body weight gain and prevents hyperglycemia in HFD-mice

Metformin is widely used as a preventative medicine for type 2 diabetes as well as cancer. [45-47] Instead of treatment with metformin 2 months after HFD-feeding and the presence of hyperglycemia, metformin was administered at the beginning of HFD-feeding to determine whether metformin was able to prevent HFD-induced retinal dysfunction. Mice fed with a HFD for two weeks showed a significant weight gain compared to control (Fig. 8A, *). However, mice fed a HFD and treated with metformin concurrently (HFD + Pre-met) did not show a significant weight gain until week 9 (Fig. 8A, #), and this group had a significantly lower body weight from weeks 11-19 compared to HFD-mice without the metformin intervention (Fig. 8A, &). In addition, HFD-mice treated with metformin concurrently did not become hyperglycemic (Fig. 8B) and did not show glucose intolerance (Fig. 8C), nor display insulin resistance (Fig. 8D) compared to the HFD-mice after 3 months of the feeding-regimen.

Concurrent treatment of metformin does not prevent HFD-induced retinal dysfunction

Retinal light responses were measured 3 months after mice were fed normal chow (control), a HFD, and a HFD with daily metformin treatment concurrently from the beginning (HFD + Pre-met). As previously observed, HFD-mice show decreased a- and b- wave amplitudes and delayed a- and b-wave implicit times compared to control mice (Fig. 9A). HFD-mice that were treated with metformin from the beginning (HFD+Pre-met) also had decreased a- and b-wave amplitudes and delayed a- and b-wave implicit times compared to control mice (Fig. 9A). The oscillatory potential responses for both HFD and HFD-mice treated with metformin (HFD + Pre-met) were worsen after 3 months of HFD-feeding regimen (Fig. 9C).

1 month of concurrent metformin treatment does not prevent HFD-induced changes in cell signaling in the retina

Previously, we showed that HFD mice with metformin treatment starting after 2 months of the diet regimen and subsequently treated with metformin for another 4 months (HFD + Met group) had reversed changes in cell signaling molecules that were caused by HFD in the retina (Fig. 5). We examined what early changes in cell signaling that HFD regimen would induce, and if treatment of metformin concurrently with HFD from the beginning would prevent the HFD-induced changes in the retina after HFD-regimen for only 1 month. We quantified the changes in the inner segments of photoreceptors and across the retinal layers (from the outer segment of photoreceptors to

the ganglion cell layer) in the retinal sections from mice fed with standard chow (Con), a HFD, and a HFD with daily metformin treatment (HFD + Pre-met). There was no significant difference in the fluorescent intensities of pAKT (Fig. 10A, 11A), Total AKT (Fig. 10B, 11B), pAMPK (Fig. 10C, 11C), and Total ERK (Fig. 10F, 11F) among the three groups (Fig. 11A, B, C, F). The fluorescent intensities for Total AMPK (Fig. 10D) were increased in the HFD+Pre-met group in the inner segment compared to control mice (Fig. 11D, left panel). The fluorescent intensities for pERK (Fig. 10E, 11E), pP65 (Fig. 10G, 10G), Total P65 (Fig. 10H, 11H) and the L-type voltage-gated calcium channel Cav1.3 (LTCC; Fig. 10I, 11I) were increased in both the HFD and HFD+Pre-met groups in the inner segment compared to control mice (Fig. 11E, G, H, I). There was no significant difference in fluorescent intensities among the three groups when the fluorescent intensities were analyzed across all retinal layers (Fig. 11).

CHAPTER IV

DISCUSSION AND CONCLUSION*

We examined the effects of administering metformin, an anti-hyperglycemic agent, as a preventative and recovery drug on retinal function and physiology in HFD-induced diabetic mice. We hypothesized that controlling systemic glycemia with metformin could recover HFD-induced retinal dysfunction. To simulate clinical settings of human diabetic patients, we started the metformin treatments in these HFD-mice after hyperglycemia was detected. As seen in human patients where the ERG OPs are more sensitive to diabetic stress, [48, 49] we observed that one month after HFD regimen, the HFD-mice had decreased OPs and delayed OP implicit times, even though these HFD-mice had not yet developed systemic hyperglycemia. These data indicate that retinal function might be compromised during pre-diabetic conditions preceding systemic hyperglycemia. With the development of diabetes, both ERG a- and b-waves were dampened after 2 months of HFD, which were concurrent with the development of hyperglycemia. Treatment with metformin significantly decelerated weight gain and controlled systemic blood glucose levels in HFD-mice, but it was not able to restore retinal function. The ERG OP amplitudes were further decreased and implicit time was further delayed in metformin-treated HFD-mice (HFD+Met) compared to HFD-mice without metformin intervention.

---

*Reprinted with permission from Kim AJ, Chang JY-A, Shi L, Chang RC-A, Ko ML, Ko GY-P. The effects of metformin on obesity-induced dysfunctional retinas. *Invest Ophthalmol Vis Sci*. 2017;58:106-118. Copyright 2017 Association for Research in Vision and Ophthalmology

In a recent report, [23] mice fed with a HFD containing 42% fat calories developed diabetes by 6 months of the diet regimen, and by 12 months, decreased OPs with delayed OP implicit times, as well as vascular complications including atrophic capillaries and pericyte ghosts are apparent. Interestingly, there was no significant change in the ERG a- and b-waves recorded from these HFD-mice. [23] We consistently observe that mice fed with a HFD containing 59.4% fat calories develop glucose intolerance and insulin resistance at the end of 3 months of the HFD regimen, [24, 25] which is consistent with other reports using the HFD with the same fat calories. [50-53] These HFD-mice have significant weight gain only 2 weeks after the diet regimen compared to control mice. As we previously reported, [24, 25] the ERG a- and b-waves in these HFD-mice have decreased amplitudes and delayed implicit times. We further demonstrated that OPs were affected in the HFD-mice even prior to systemic hyperglycemia. These results indicate that the dietary fat content affects the temporal progression of DR. Mice fed a HFD with 42% fat calories show decreased OPs after 1 year, while we show that OP deficiencies are evident only after 1 month of HFD with 59.4% fat calories. More studies are necessary to show whether the increased fat concentration in diet speeds up obesity and type 2 diabetes or if the fat percentage has a direct impact on the neural retina.

Despite the inability to recover retinal function, metformin had significant effects on several cell-signaling proteins in the retina that were altered by HFD. In context of the pathogenesis of DR, the phosphoinositide 3-kinase-AKT (PI3K-AKT) pathway has been shown to regulate angiogenesis. [54] Previously, we showed that HFD-induced type 2 diabetic retinas have reduced pAKT that is also seen in STZ-induced type 1 diabetic

mice. [55] We found that metformin treatments restored pAKT and increased AMPK and pAMPK in HFD-mouse retinas. AMPK is a cellular energy sensor, and activated AMPK further stimulates catabolic processes for increasing ATP production. [38] In muscles, AMPK activates the PI3K-AKT pathway that leads to increased glucose uptake into the muscle cells. [56] We previously showed that activation of AMPK leads to activation of AKT and its downstream signaling in the avian retina. [57] Metformin is known to up-regulate the expression and activation of AMPK in the kidney, [39] adipose tissue, [40, 41] and heart. [42] Hence, the effects of metformin on pAKT could be a downstream effect from its activation of AMPK-dependent signaling.

In addition, increased activation/phosphorylation of ERK (pERK) is correlated with the presence of pro-inflammatory cytokines. [58] Activation of ERK is involved in the up-regulation of VEGF, an angiogenic protein that causes microvascular complications and neovascularization in DR. [59, 60] We showed that phosphorylation of ERK was increased in the retinas of HFD-mice, and treatment with metformin reduced pERK in HFD-mouse retina. Furthermore, HFD mouse retinas had increased expression of pP65 compared to controls, which was reduced in retinas of metformin treated HFD-mice. Obesity is known to induce systemic inflammation, [61-63] but induction of systemic inflammation does not correlate with retinal inflammation. [64] Previously, we also analyzed the status of intra-ocular inflammation from the vitreous and lens. [65] The expression of pro-inflammatory cytokines in HFD-mice was increased, and metformin was able to reverse HFD-induced intra-ocular inflammation. Although it was unable to

reverse HFD-induced retinal dysfunction and neovascularization, metformin was able to reverse intra-ocular inflammation and HFD-induced effects on retinal proteins.

In addition, metformin has successfully acted as a protective drug in various disease models when used to pre-treat animals prior to the induction of diseases, including acute kidney injury [66] and cerebral forebrain ischemia. [67, 68] Since metformin treatment following hyperglycemia was unable to reverse numerous HFD-induced changes in the retina, we hypothesized that metformin is more effective given at a pre-diabetic or non-diabetic stage as a preventive strategy rather than as a treatment for diabetic retinas. Treatment with metformin in the beginning concurrent with HFD not only caused a delayed weight gain in HFD-mice, but also prevented the development of hyperglycemia. Nevertheless, both HFD mice and HFD-mice treated with metformin concurrently (HFD + Pre-met) showed deficiencies in retinal light responses even after 3 months of treatment. These data show that decreased retinal light responses as measured by ERG are not a result of hyperglycemia, but rather due to other obesity-induced changes such as dyslipidemia or inflammation. Furthermore, immunohistochemical staining of retinas from mice with 1 month of HFD or HFD with metformin treatment (HFD + Pre-met) showed that metformin was unable to reverse HFD-induced changes in cell signaling. 1 month of HFD-feeding showed increases in pERK, pP65, Total P65, and LTCC Cav1.3 expressions in the retinal photoreceptors. However, treatment of metformin for 1 month was not able to act as a protective agent for these changes. The increases in pP65 and Total P65 indicate the presence of inflammation in the retina even when blood glucose levels are controlled by metformin, showing that inflammation is

not an effect of hyperglycemia. It is possible that it will take a longer time for metformin treatments to reverse HFD-induced retinal inflammation, while metformin could effectively reverse or prevent systemic hyperglycemia within 1 month. While metformin is not metabolized in the body, it is quickly excreted from the body, but after long-term treatments with metformin, it may accumulate in the body and requires longer clearance times. [69, 70]

Lastly, after 1 month treatment with metformin, we observed an increase in the fluorescent intensities of total AMPK in the photoreceptors. AMPK acts as an energy sensor by being activated or inactivated depending on the AMP to ATP ratio in the cell. [71] Metformin has been identified as an activator of the AMPK pathway in numerous cell types including hepatocytes, [72, 73] endothelial cells, [74] cardiomyocytes, [75] cancer cells, [76] and adipose tissue. [41] In photoreceptors, we found that the expression of total AMPK was increased after 1 month of metformin treatment, while there is a significant increase in pAMPK after 4 months of metformin treatment. A recent study shows that metformin administration through intraperitoneal injection also increases pAMPK in the mouse retinas.[77] Thus, the activation of AMPK by metformin in the neural retina is a primary effect, since metformin is able to reach the neural retina through blood circulation regardless of its routes of administration.

In summary, long-term treatment with metformin successfully reversed hyperglycemia and decreased retinal inflammation in HFD-mice, but was unable to restore retinal light responses. Early treatment with metformin prevented HFD-mice

from becoming hyperglycemic, but it did not prevent HFD-induced retinal dysfunction and changes in cell signaling.

Following chronic hyperglycemia, changes in the normal metabolic state including inflammation, oxidative stress, and dyslipidemia have been hypothesized as major contributors to proliferative diabetic retinopathy.[78, 79] Besides its main function as an anti-hyperglycemia agent, metformin addresses these secondary metabolic disturbances in addition to controlling systemic blood glucose levels within a single treatment. Our data shows metformin effectively reduces intra-ocular inflammation, but retinal function was unable to be recovered and its dysfunction could not be prevented with prior treatment. This evidence challenges predominant theories that a pro-inflammatory state in the retina is driving the downstream metabolic changes leading to neovascularization and proliferation. Despite metformin's beneficial effects on the overall metabolic state of the retina, retinal dysfunction was unable to be prevented. Our specific use of metformin was to target hyperglycemia, the initiator of metabolic dysfunction. However, our data showed that recovery of hyperglycemia did not recover retinal function and further demonstrated that mice that never become hyperglycemic still acquire retinal dysfunction. This data proposes that hyperglycemia and inflammation may not be the causes for retinal dysfunction caused by obesity. Attempts to stall the development of DR pathogenesis have been widely unsuccessful, largely because numerous metabolic changes occur following chronic hyperglycemia. Targeting single downstream signaling pathways have failed to prevent angiogenesis, and we show that controlling two major proposed contributors in hyperglycemia and inflammation

through metformin does not prevent retinal dysfunction. There is a critical need to pinpoint the source of retinal dysfunction and neovascularization or targeting a metabolic mechanism that can deter the pathogenesis of DR.

In a high-fat-diet obesity model, another potential contributor in driving retinal dysfunction and neovascularization is oxidative stress. Metformin administered to diabetic rats reduces oxidative stress in plasma, the aorta, and the kidney.[80] Although metformin does show capabilities in reducing oxidative stress, further experiments are necessary to verify its anti-oxidative capabilities specifically in the retina. Since mitochondrial oxidative phosphorylation and the nicotinamide adenine dinucleotide phosphate- (NADPH) oxidase (NOX) system are the two major sources of oxidative stress, it would be beneficial to know if metformin also has an effect on limiting the production of reactive oxygen species from these metabolic producers. Immediate experiments such as IHC staining of key markers such as superoxide dismutase 2 (SOD2) and NADPH-oxidase 2 (NOX2) on metformin treated HFD-mice may indicate metformin's potential on reducing oxidative stress. In addition, experiments using the Seahorse XF analyzer would be able to measure energy production produced from oxidative phorphorylation and glycolysis. Using the Seahorse XF analyzer, experiments with photoreceptors and/or endothelial cells in high glucose conditions (30 mM) can be treated with metformin to see if supplementation with this drug can reduce the overproduction of reactive oxygen species as a byproduct of mitochondrial oxidative phosphorylation. Furthermore, fluorescence ROS assays can be done on cultured

photoreceptors and/or endothelial cells with and without metformin treatment to measure the presence of different types of reactive oxygen species through fluorescence.

Although our data indicates that 4 months of metformin treatment does not have a statistical difference in neovascularization in the peripheral eye compared to high-fat-diet fed mice, it is possible we are making a statistical type II error because the amount of mice included in our analysis is only n=4. Although, the ANOVA p-value comparing the HFD and HFD+metformin group is 0.2 and we fail to reject the null hypothesis, the range of values especially in the # of branch points parameter shoes a tight range of values in the metformin treated mice group compared to the HFD group indicating that metformin is having some effect on delaying or decreasing neovascularization. Metformin has been reported to reduce VEGFR2 activation in Strepzotocin(STZ)-induced diabetic mice.[81] We have also shown that the amount of VEGF in the lens and vitreous of mice treated with metformin is comparable to control levels and decreased compared to HFD mice. [65] Despite having conflicting reports in cancer-related angiogenesis, [82] metformin has shown to have anti-angiogenic effects in the oxygen-induced retinopathy mouse model with reduced vasculature and expression of VEGFR2. [83] Further experiments are necessary to observe if the high-fat-diet model with metformin treatment also has similar effects of VEGF and VEGFR2 expression after metformin treatment. Before *in vivo* experiments with metformin treatments are done to check the possibility of a type II statistical error, western blot or IHC experiments probing for VEGF and VEGFR2 protein expression would show if metformin treatment similarly has effects in reducing VEGFR2 in the high-fat-diet model and thus be

potentially alleviating angiogenesis. Metformin treatment on endothelial cells has previously been completed, but the conditions of high-fat-diet have not been replicated. Further *in vitro* experiments on endothelial cells can be done to see if a high-fat-diet like conditions shows proliferation and migration in endothelial cells. Using high glucose conditions or administration of palmitate to emulate the increase of glucose levels or free fatty acids in HFD conditions, experiments on endothelial cells such as the MTT assay or scratch assay can be done with or without metformin treatment to see if metformin could have anti-angiogenic effects specifically on endothelial cells in HFD-like conditions.

Despite metformin's numerous beneficial effects on the retina, a potential reason why the overall function in the retina does not recover is due to a phenomenon called "metabolic memory." Metabolic memory is the persistence of hyperglycemia-induced changes even after reversing back to normoglycemia. [84] Metabolic memory was first observed in dogs, [85] but it has also been documented in STZ-induced diabetic rats. [86, 87] Here we show that metformin was able to reverse blood glucose levels back to the normal level in HFD-mice, but continued treatments with metformin could not restore the retinal function, which indicates that retina might have a strong "metabolic memory" to be overcome. Although metformin was able to reverse systemic glucose levels and inflammation, it is possible that reversal of hyperglycemia and inflammation might not be able to completely stop or restore HFD-induced dysfunctional retina. Hence, it may require a combination therapy in addition to anti-hyperglycemic, anti-inflammatory, plus other treatments to reverse obesity-induced DR.

In addition, vascular endothelial growth factor (VEGF) is a growth factor that is mainly implicated in its role on endothelial cells in stimulating angiogenesis. After binding to its tyrosine kinase receptors, VEGF stimulates the RAS-ERK and PI3K-AKT pathways for cell proliferation. The immunohistochemistry data after 4 months of metformin treatment indicates decreased ERK activation compared to only HFD-fed mice. However, HFD-fed mice had decreased AKT activation and metformin treated HFD-mice had further increased AKT activation back to control levels. In regards to angiogenesis, this increased AKT activation may be contributing to increased angiogenesis in metformin treatment and interfering with other anti-angiogenic responses such as decreased ERK signaling activation. To verify that activation of the PI3K-AKT pathway in metformin treated mice is not restricting metformin's potential in limiting angiogenesis, HFD and HFD + metformin treatment can be administered to endothelial specific AKT knockout mice and similarly tested for neovascularization through fluorescein angiography. If these AKT knockout mice given HFD and metformin treatment show significantly decreased neovascularization compared to HFD-mice, metformin plus AKT pathway inhibitors may be a potential route for treatment or prevention of angiogenesis.

The data presented in this thesis challenges the common conception that controlling hyperglycemia and/or inflammation will deter the progression of diabetic retinopathy. Metformin is shown to control systemic hyperglycemia and reduce intra-ocular inflammation but do not show statistically significant improvements in retinal function or neovascularization. Further experiments on metformin's effects on the retina

can reveal what signaling pathways were unaffected or exacerbated through metformin treatment and provide insight into potential new therapies in preventing or delaying diabetic retinopathy.

REFERENCES

1. Wild S, Roglic G, Green A, Sicree R, King H. Global prevalence of diabetes: estimates for the year 2000 and projections for 2030. *Diabetes Care* 2004;27:1047-1053.

2. American Diabetes A. Standards of medical care in diabetes--2013. *Diabetes Care* 2013;36 Suppl 1:S11-66.

3. The effect of intensive treatment of diabetes on the development and progression of long-term complications in insulin-dependent diabetes mellitus. The Diabetes Control and Complications Trial Research Group. *N Engl J Med* 1993;329:977-986.

4. Effect of intensive blood-glucose control with metformin on complications in overweight patients with type 2 diabetes (UKPDS 34). UK Prospective Diabetes Study (UKPDS) Group. *Lancet* 1998;352:854-865.

5. Song S, Andrikopoulos S, Filippis C, Thorburn AW, Khan D, Proietto J. Mechanism of fat-induced hepatic gluconeogenesis: effect of metformin. *Am J Physiol Endocrinol Metab* 2001;281:E275-282.

6. Inzucchi SE, Bergenstal RM, Buse JB, et al. Management of hyperglycaemia in type 2 diabetes: a patient-centered approach. Position statement of the American Diabetes Association (ADA) and the European Association for the Study of Diabetes (EASD). *Diabetologia* 2012;55:1577-1596.

7. Yu S, Schwab P, Bian B, Radican L, Tunceli K. Use of add-on treatment to metformin monotherapy for patients with type 2 diabetes and suboptimal glycemic control: a U.S. database study. *J Manag Care Spec Pharm* 2016;22:272-280.

8. Stumvoll M, Nurjhan N, Perriello G, Dailey G, Gerich JE. Metabolic effects of metformin in non-insulin-dependent diabetes mellitus. *N Engl J Med* 1995;333:550-554.

9. Malin SK, Kashyap SR. Effects of metformin on weight loss: potential mechanisms. *Curr Opin Endocrinol Diabetes Obes* 2014;21:323-329.

10. Diabetes Prevention Program Research G. Long-term safety, tolerability, and weight loss associated with metformin in the Diabetes Prevention Program Outcomes Study. *Diabetes Care* 2012;35:731-737.

11. Diabetes Prevention Program Research G, Knowler WC, Fowler SE, et al. 10-year follow-up of diabetes incidence and weight loss in the Diabetes Prevention Program Outcomes Study. *Lancet* 2009;374:1677-1686.

12. Guigas B, Bertrand L, Taleux N, et al. 5-Aminoimidazole-4-carboxamide-1-beta-D-ribofuranoside and metformin inhibit hepatic glucose phosphorylation by an AMP-activated protein kinase-independent effect on glucokinase translocation. *Diabetes* 2006;55:865-874.

13. Valsamakis G, Lois K, Kumar S, Mastorakos G. Metabolic and other effects of pioglitazone as an add-on therapy to metformin in the treatment of polycystic ovary syndrome (PCOS). *Hormones (Athens)* 2013;12:363-378.

14. Alhaider AA, Korashy HM, Sayed-Ahmed MM, Mobark M, Kfoury H, Mansour MA. Metformin attenuates streptozotocin-induced diabetic nephropathy in rats through modulation of oxidative stress genes expression. *Chem Biol Interact* 2011;192:233-242.

15. Wile DJ, Toth C. Association of metformin, elevated homocysteine, and methylmalonic acid levels and clinically worsened diabetic peripheral neuropathy. *Diabetes Care* 2010;33:156-161.

16. Cunha-Vaz J, Ribeiro L, Lobo C. Phenotypes and biomarkers of diabetic retinopathy. *Prog Retin Eye Res* 2014;41:90-111.

17. Fong DS, Aiello L, Gardner TW, et al. Retinopathy in diabetes. *Diabetes Care* 2004;27 Suppl 1:S84-87.

18. Winzell MS, Ahren B. The high-fat diet-fed mouse: a model for studying mechanisms and treatment of impaired glucose tolerance and type 2 diabetes. *Diabetes* 2004;53 Suppl 3:S215-219.

19. Fellmann L, Nascimento AR, Tibirica E, Bousquet P. Murine models for pharmacological studies of the metabolic syndrome. *Pharmacol Ther* 2013;137:331-340.

20. Ahren B, Simonsson E, Scheurink AJ, Mulder H, Myrsen U, Sundler F. Dissociated insulinotropic sensitivity to glucose and carbachol in high-fat diet-induced insulin resistance in C57BL/6J mice. *Metabolism* 1997;46:97-106.

21. Weisberg SP, McCann D, Desai M, Rosenbaum M, Leibel RL, Ferrante AW, Jr. Obesity is associated with macrophage accumulation in adipose tissue. *J Clin Invest* 2003;112:1796-1808.

22. Vinores SA, Campochiaro PA, May EE, Blaydes SH. Progressive ultrastructural damage and thickening of the basement membrane of the retinal pigment epithelium in spontaneously diabetic BB rats. *Exp Eye Res* 1988;46:545-558.

23. Rajagopal R, Bligard GW, Zhang S, Yin L, Lukasiewicz P, Semenkovich CF. Functional deficits precede structural lesions in mice with high-fat diet-induced diabetic retinopathy. *Diabetes* 2016;65:1072-1084.

24. Chang RC, Shi L, Huang CC, et al. High-Fat Diet-Induced Retinal Dysfunction. *Invest Ophthalmol Vis Sci* 2015;56:2367-2380.

25. Shi L, Kim AJ, Chang RC, et al. Deletion of miR-150 exacerbates retinal vascular overgrowth in high-fat-diet induced diabetic mice. *PLoS One* 2016;11:e0157543.

26. Knowler WC, Barrett-Connor E, Fowler SE, et al. Reduction in the incidence of type 2 diabetes with lifestyle intervention or metformin. *N Engl J Med* 2002;346:393-403.

27. Zinman B, Harris SB, Gerstein HC, et al. Preventing type 2 diabetes using combination therapy: design and methods of the CAnadian Normoglycaemia Outcomes Evaluation (CANOE) trial. *Diabetes Obes Metab* 2006;8:531-537.

28. Zudaire E, Gambardella L, Kurcz C, Vermeren S. A computational tool for quantitative analysis of vascular networks. *PLoS One* 2011;6:e27385.

29. Pardue MT, Barnes CS, Kim MK, et al. Rodent hyperglycemia-induced inner retinal deficits are mirrored in human diabetes. *Transl Vis Sci Technol* 2014;3:6.

30. Shirao Y, Kawasaki K. Electrical responses from diabetic retina. *Prog Retin Eye Res* 1998;17:59-76.

31. Yonemura D, Aoki T, Tsuzuki K. Electroretinogram in diabetic retinopathy. *Arch Ophthalmol* 1962;68:19-24.

32. Dilly AK, Rajala RV. Insulin growth factor 1 receptor/PI3K/AKT survival pathway in outer segment membranes of rod photoreceptors. *Invest Ophthalmol Vis Sci* 2008;49:4765-4773.

33. Li G, Rajala A, Wiechmann AF, Anderson RE, Rajala RV. Activation and membrane binding of retinal protein kinase Balpha/Akt1 is regulated through light-dependent generation of phosphoinositides. *J Neurochem* 2008;107:1382-1397.

34. Chang L, Chiang SH, Saltiel AR. Insulin signaling and the regulation of glucose transport. *Mol Med* 2004;10:65-71.

35. Barros LF, Deitmer JW. Glucose and lactate supply to the synapse. *Brain Res Rev* 2010;63:149-159.

36. Lopez L, Sannita WG. Glucose availability and the electrophysiology of the human visual system. *Clin Neurosci* 1997;4:336-340.

37. Cobb MH. MAP kinase pathways. *Prog Biophys Mol Biol* 1999;71:479-500.

38. Hardie DG. AMP-activated/SNF1 protein kinases: conserved guardians of cellular energy. *Nat Rev Mol Cell Biol* 2007;8:774-785.

39. Kim D, Lee JE, Jung YJ, et al. Metformin decreases high-fat diet-induced renal injury by regulating the expression of adipokines and the renal AMP-activated protein kinase/acetyl-CoA carboxylase pathway in mice. *Int J Mol Med* 2013;32:1293-1302.

40. Li A, Zhang S, Li J, Liu K, Huang F, Liu B. Metformin and resveratrol inhibit Drp1-mediated mitochondrial fission and prevent ER stress-associated NLRP3 inflammasome activation in the adipose tissue of diabetic mice. *Mol Cell Endocrinol* 2016.

41. Luo T, Nocon A, Fry J, et al. AMPK activation by metformin suppresses abnormal adipose tissue extracellular matrix remodeling and ameliorates insulin resistance in obesity. *Diabetes* 2016.

42. Lai YC, Tabima DM, Dube JJ, et al. SIRT3-AMP-activated protein kinase activation by nitrite and metformin improves hyperglycemia and normalizes pulmonary hypertension associated with heart failure with preserved ejection fraction. *Circulation* 2016;133:717-731.

43. Saisho Y. Metformin and inflammation: its potential beyond glucose-lowering effect. *Endocr Metab Immune Disord Drug Targets* 2015;15:196-205.

44. Karin M, Greten FR. NF-kappaB: linking inflammation and immunity to cancer development and progression. *Nat Rev Immunol* 2005;5:749-759.

45. Akinyeke T, Matsumura S, Wang X, et al. Metformin targets c-MYC oncogene to prevent prostate cancer. *Carcinogenesis* 2013;34:2823-2832.

46. Doggrell SA. Metformin & lifestyle intervention prevent Type 2 diabetes: lifestyle intervention has the greater effect. *Expert Opin Pharmacother* 2002;3:1011-1013.

47. Louro TM, Matafome PN, Nunes EC, da Cunha FX, Seica RM. Insulin and metformin may prevent renal injury in young type 2 diabetic Goto-Kakizaki rats. *Eur J Pharmacol* 2011;653:89-94.

48. Bresnick GH, Palta M. Predicting progression to severe proliferative diabetic retinopathy. *Arch Ophthalmol* 1987;105:810-814.

49. Bresnick GH, Palta M. Oscillatory potential amplitudes. Relation to severity of diabetic retinopathy. *Arch Ophthalmol* 1987;105:929-933.

50. Guo T, Woo SL, Guo X, et al. Berberine ameliorates hepatic steatosis and suppresses liver and adipose tissue inflammation in mice with diet-induced obesity. *Sci Rep* 2016;6:22612.

51. Woo SL, Xu H, Li H, et al. Metformin ameliorates hepatic steatosis and inflammation without altering adipose phenotype in diet-induced obesity. *PLoS One* 2014;9:e91111.

52. Ying W, Tseng A, Chang RC, et al. MicroRNA-223 is a crucial mediator of PPARgamma-regulated alternative macrophage activation. *J Clin Invest* 2015;125:4149-4159.

53. Zhuang G, Meng C, Guo X, et al. A novel regulator of macrophage activation: miR-223 in obesity-associated adipose tissue inflammation. *Circulation* 2012;125:2892-2903.

54. Ackah E, Yu J, Zoellner S, et al. Akt1/protein kinase Balpha is critical for ischemic and VEGF-mediated angiogenesis. *J Clin Invest* 2005;115:2119-2127.

55. Jiang T, Chang Q, Cai J, Fan J, Zhang X, Xu G. Protective effects of melatonin on retinal inflammation and oxidative stress in experimental diabetic retinopathy. *Oxid Med Cell Longev* 2016;2016:3528274.

56. Sajan MP, Bandyopadhyay G, Miura A, et al. AICAR and metformin, but not exercise, increase muscle glucose transport through AMPK-, ERK-, and PDK1-

dependent activation of atypical PKC. *Am J Physiol Endocrinol Metab* 2010;298:E179-192.

57. Huang CC, Shi L, Lin CH, Kim AJ, Ko ML, Ko GY. A new role for AMP-activated protein kinase in the circadian regulation of L-type voltage-gated calcium channels in late-stage embryonic retinal photoreceptors. *J Neurochem* 2015;135:727-741.

58. Busik JV, Mohr S, Grant MB. Hyperglycemia-induced reactive oxygen species toxicity to endothelial cells is dependent on paracrine mediators. *Diabetes* 2008;57:1952-1965.

59. Hu J, Li T, Du S, et al. The MAPK signaling pathway mediates the GPR91-dependent release of VEGF from RGC-5 cells. *Int J Mol Med* 2015;36:130-138.

60. Jin J, Yuan F, Shen MQ, Feng YF, He QL. Vascular endothelial growth factor regulates primate choroid-retinal endothelial cell proliferation and tube formation through PI3K/Akt and MEK/ERK dependent signaling. *Mol Cell Biochem* 2013;381:267-272.

61. Kim MS, Yamamoto Y, Kim K, et al. Regulation of diet-induced adipose tissue and systemic inflammation by salicylates and pioglitazone. *PLoS One* 2013;8:e82847.

62. Ying W, Kanameni S, Chang CA, et al. Interferon tau alleviates obesity-induced adipose tissue inflammation and insulin resistance by regulating macrophage polarization. *PLoS One* 2014;9:e98835.

63. Ying W, Tseng A, Chang RC, et al. miR-150 regulates obesity-associated insulin resistance by controlling B cell functions. *Sci Rep* 2016;6:20176.

64. Tamura H, Kiryu J, Miyamoto K, et al. In vivo evaluation of ocular inflammatory responses in experimental diabetes. *Br J Ophthalmol* 2005;89:1052-1057.

65. Kim AJ, Chang JY, Shi L, Chang RC, Ko ML, Ko GY. The effects of metformin on obesity-induced dysfunctional retinas. *Invest Ophthalmol Vis Sci* 2017;58:106-118.

66. Li J, Gui Y, Ren J, et al. Metformin protects against cisplatin-induced tubular cell apoptosis and acute kidney injury via AMPKalpha-regulated autophagy induction. *Sci Rep* 2016;6:23975.

67. Ashabi G, Khalaj L, Khodagholi F, Goudarzvand M, Sarkaki A. Pre-treatment with metformin activates Nrf2 antioxidant pathways and inhibits inflammatory responses through induction of AMPK after transient global cerebral ischemia. *Metab Brain Dis* 2015;30:747-754.

68. Ghadernezhad N, Khalaj L, Pazoki-Toroudi H, Mirmasoumi M, Ashabi G. Metformin pretreatment enhanced learning and memory in cerebral forebrain ischaemia: the role of the AMPK/BDNF/P70SK signalling pathway. *Pharm Biol* 2016;1-9.

69. Graham GG, Punt J, Arora M, et al. Clinical pharmacokinetics of metformin. *Clin Pharmacokinet* 2011;50:81-98.

70. Kajbaf F, Bennis Y, Hurtel-Lemaire AS, Andrejak M, Lalau JD. Unexpectedly long half-life of metformin elimination in cases of metformin accumulation. *Diabet Med* 2016;33:105-110.

71. Lage R, Dieguez C, Vidal-Puig A, Lopez M. AMPK: a metabolic gauge regulating whole-body energy homeostasis. *Trends Mol Med* 2008;14:539-549.

72. Cao J, Meng S, Chang E, et al. Low concentrations of metformin suppress glucose production in hepatocytes through AMP-activated protein kinase (AMPK). *J Biol Chem* 2014;289:20435-20446.

73. Meng S, Cao J, He Q, et al. Metformin activates AMP-activated protein kinase by promoting formation of the alphabetagamma heterotrimeric complex. *J Biol Chem* 2015;290:3793-3802.

74. Yu JW, Deng YP, Han X, Ren GF, Cai J, Jiang GJ. Metformin improves the angiogenic functions of endothelial progenitor cells via activating AMPK/eNOS pathway in diabetic mice. *Cardiovasc Diabetol* 2016;15:88.

75. Hu M, Ye P, Liao H, Chen M, Yang F. Metformin protects H9C2 cardiomyocytes from high-glucose and hypoxia/reoxygenation injury via inhibition of reactive oxygen species generation and inflammatory responses: role of AMPK and JNK. *J Diabetes Res* 2016;2016:2961954.

76. Sun Y, Tao C, Huang X, et al. Metformin induces apoptosis of human hepatocellular carcinoma HepG2 cells by activating an AMPK/p53/miR-23a/FOXA1 pathway. *Onco Targets Ther* 2016;9:2845-2853.

77. Athanasiou D, Aguila M, Opefi CA, et al. Rescue of mutant rhodopsin traffic by metformin-induced AMPK activation accelerates photoreceptor degeneration. *Hum Mol Genet* 2017.

78. Roy S, Kern TS, Song B, Stuebe C. Mechanistic insights into pathological changes in the diabetic retina: implications for targeting diabetic retinopathy. *Am J Pathol* 2017;187:9-19.

79. Chatziralli IP. The role of dyslipidemia control in the progression of diabetic retinopathy in patients with type 2 diabetes mellitus. *Diabetes Ther* 2017;209.

80. Rosen P, Wiernsperger NF. Metformin delays the manifestation of diabetes and vascular dysfunction in Goto-Kakizaki rats by reduction of mitochondrial oxidative stress. *Diabetes Metab Res Rev* 2006;22:323-330.

81. Yi QY, Deng G, Chen N, et al. Metformin inhibits development of diabetic retinopathy through inducing alternative splicing of VEGF-A. *Am J Transl Res* 2016;8:3947-3954.

82. Dallaglio K, Bruno A, Cantelmo AR, et al. Paradoxic effects of metformin on endothelial cells and angiogenesis. *Carcinogenesis* 2014;35:1055-1066.

83. Joe SG, Yoon YH, Choi JA, Koh JY. Anti-angiogenic effect of metformin in mouse oxygen-induced retinopathy is mediated by reducing levels of the vascular endothelial growth factor receptor Flk-1. *PLoS One* 2015;10:e0119708.

84. Zhang L, Chen B, Tang L. Metabolic memory: mechanisms and implications for diabetic retinopathy. *Diabetes Res Clin Pract* 2012;96:286-293.

85. Engerman RL, Kern TS. Progression of incipient diabetic retinopathy during good glycemic control. *Diabetes* 1987;36:808-812.

86. Kowluru RA, Chan PS. Metabolic memory in diabetes - from in vitro oddity to in vivo problem: role of apoptosis. *Brain Res Bull* 2010;81:297-302.

87. Kowluru RA, Kanwar M, Kennedy A. Metabolic memory phenomenon and accumulation of peroxynitrite in retinal capillaries. *Exp Diabetes Res* 2007;2007:21976.

APPENDIX

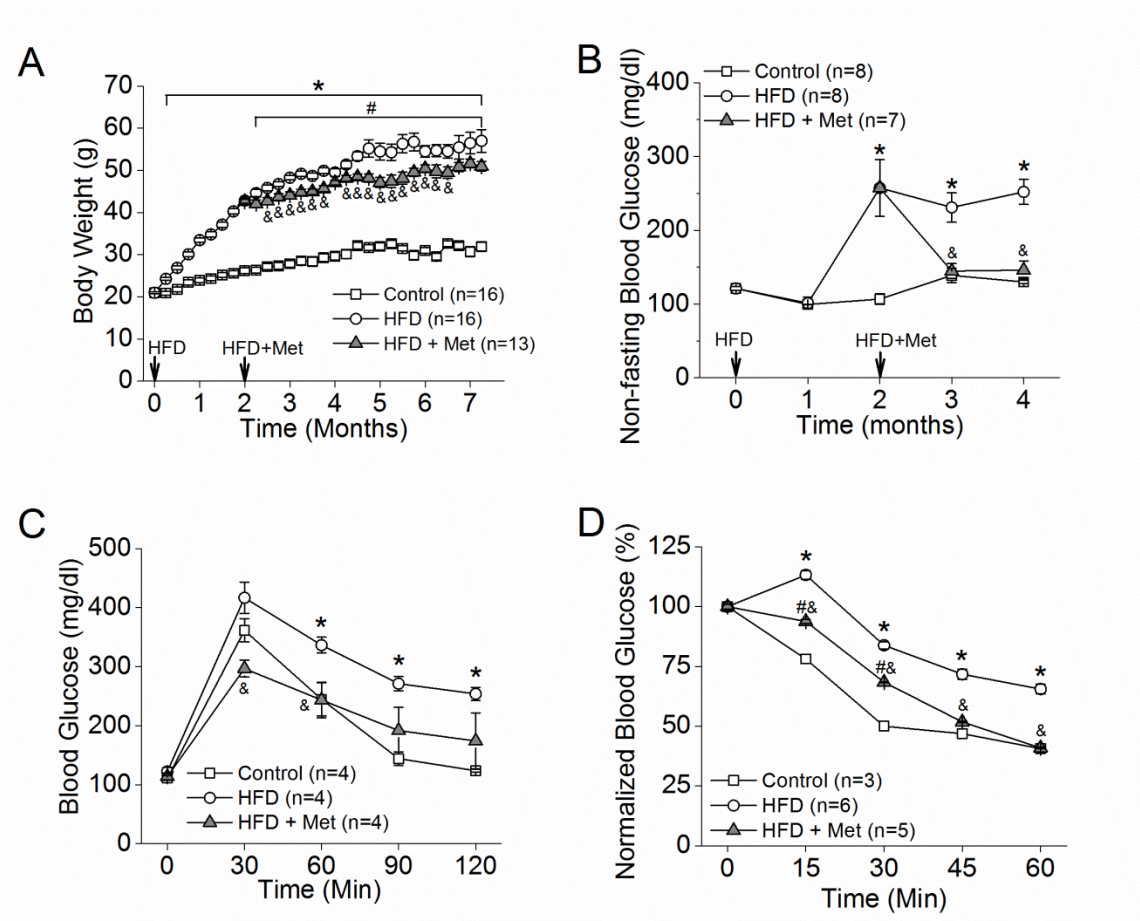

Figure 1. Metformin slows the rate of weight gain and controls diet-induced hyperglycemia in HFD mice. Mice were fed a normal chow diet (Control [open square]) or HFD (open circle). Two months after the diet regimen, half of the HFD mice were given daily oral metformin treatments (gray triangle). (A) Mice fed a HFD had significant weight gain starting 1 week after HFD-feeding compared to control mice (*). The HFD-fed mice given daily metformin (HFD+Met) showed decelerated weight gain compared to the HFD mice without metformin intervention (HFD). # indicates statistical significance between the control and HFD+Met groups. & indicates statistical significance between the HFD and HFD+Met groups. (B) HFD-fed mice had an increase of non-fasting blood glucose after 2 months of the diet regimen. Following 1 month of metformin treatment, the resting blood glucose levels of HFD+Met mice were back to control levels. (C) The glucose tolerance test and (D) insulin resistance test shows the ability of metformin to control HFD-induced hyperglycemia. $^{*,\#,\&}P < 0.05$.

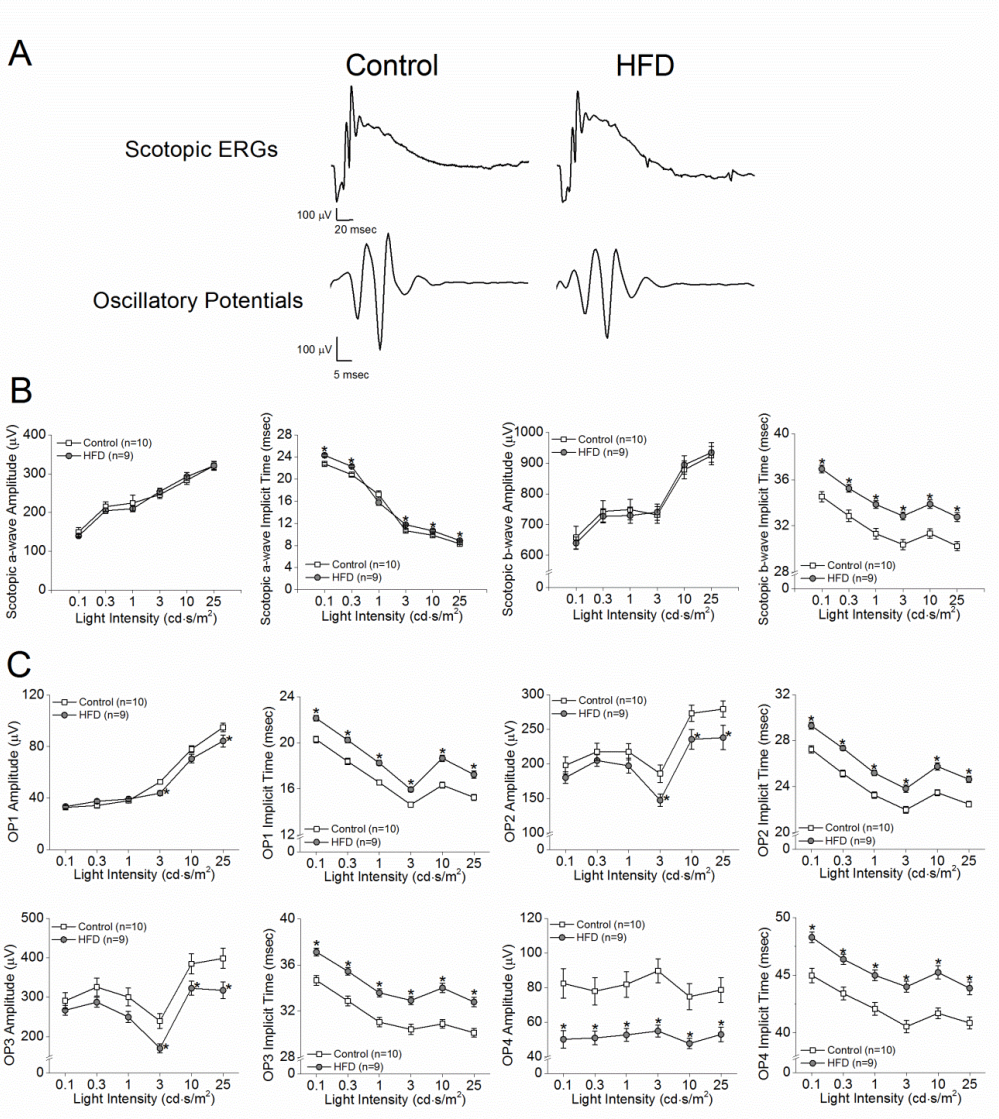

Figure 2. Scotopic ERG implicit times and oscillatory potential responses are decreased in mice given HFD for 1 month. (A) Representative scotopic ERG and oscillatory potential waveforms recorded from control and HFD-fed mice at light intensity of 25 cd·s/m^2 are shown. (B) The average scotopic ERG a- and b- wave implicit times were delayed in HFD-mice after 1 month of HFD compared to the control, but there was no difference in the ERG amplitudes. (C) The oscillatory potential amplitudes (OP1 to OP4) of HFD mice were significantly decreased and the implicit times were delayed compared to those of the control. Student's *t*-test was used for statistical analysis. *$p < 0.05$.

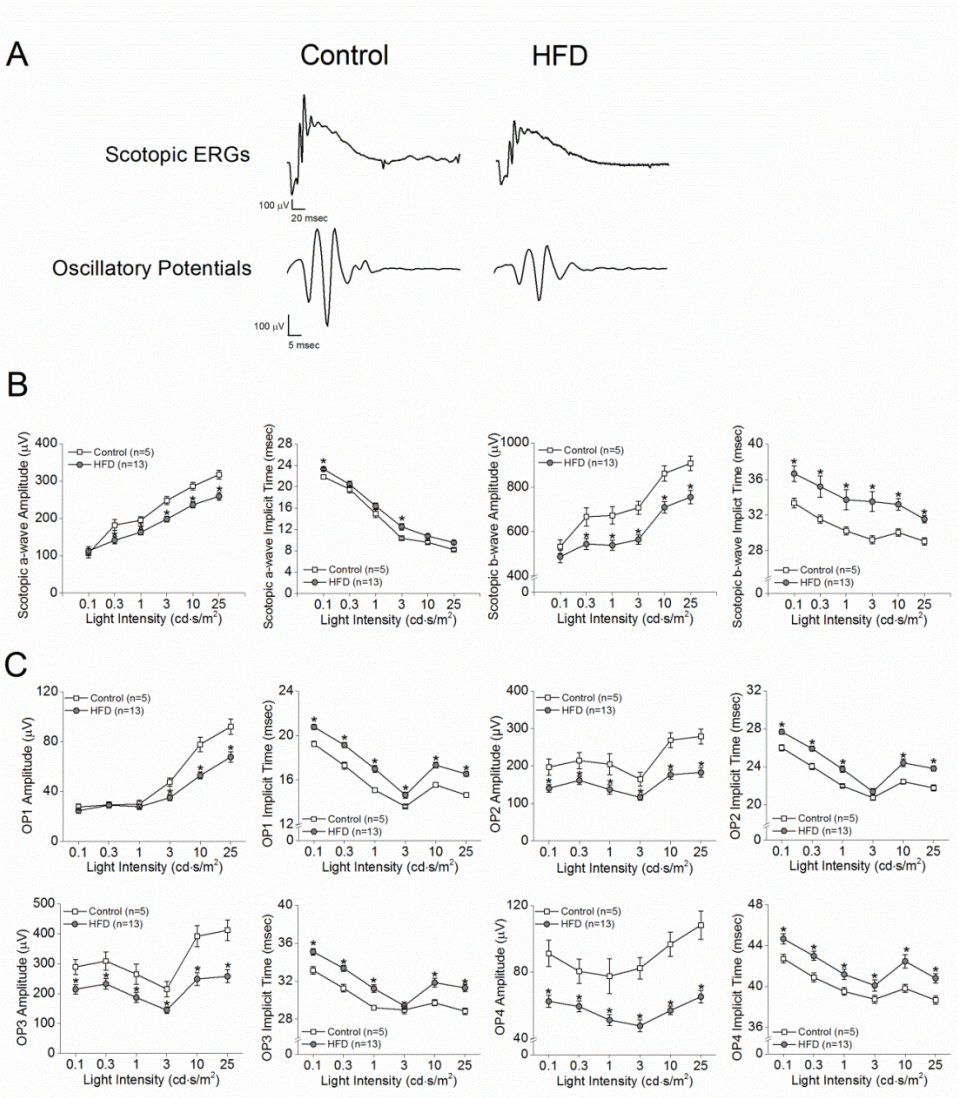

Figure 3. Scotopic ERG amplitudes, implicit times, and oscillatory potential responses are further decreased in mice given HFD for 2 months. (A) Representative scotopic ERG and oscillatory potential waveforms recorded from control and HFD-fed mice at light intensity of 25 cd·s/m^2 are shown. (B) The average scotopic ERG a- and b- wave amplitudes were decreased and implicit times delayed in mice under 2 months of HFD compared to the control. (C) The oscillatory potential amplitudes of HFD mice are also significantly decreased and the implicit times are delayed compared to the control. Student's *t*-test was used for statistical analysis. **p* < 0.05.

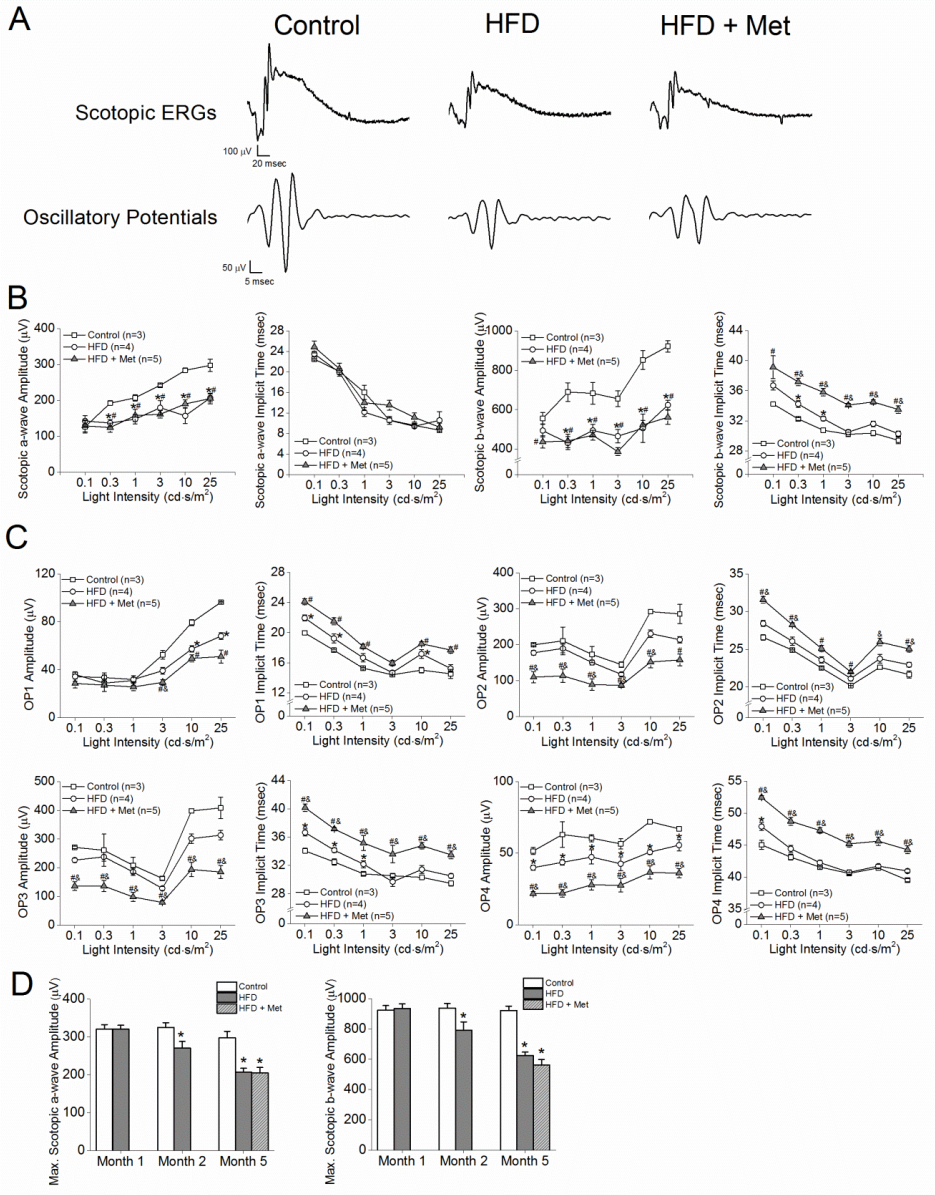

Figure 4. Metformin treatment for 3 months does not improve HFD-induced retinal deficiencies. The control **mice** were fed standard chow for 5 months (control). HFD mice were given HFD for 5 months (HFD). The HFD + metformin mice were given HFD for 5 months and metformin for the last 3 months. (A) Representative scotopic ERG and oscillatory potential waveforms recorded from control, HFD mice, and HFD-mice treated with metformin at light intensity of 25 cd·s/m^2 are shown. (B) HFD mice have decreased a- and b-wave amplitudes and delayed b-wave implicit times compared to the control (*). The HFD + metformin mice have decreased a-wave and b-wave amplitudes and delayed b-wave implicit times compared to the control (#). The HFD + metformin mice had delayed b-wave implicit times compared to those of HFD mice (&), but there was no statistical difference between the HFD and the HFD + metformin groups in a-wave amplitudes, b-wave amplitudes, and a-wave implicit times. (C) The oscillatory potential amplitudes were decreased and implicit times delayed in HFD mice compared to the control (*). The oscillatory potential amplitudes were decreased and implicit times delayed in HFD + metformin mice compared of the control (#). Furthermore, HFD + metformin mice had decreased OP amplitudes and delayed implicit times compared to the HFD mice (&). (D) Maximal scotopic a- and b-wave amplitudes are unchanged in control mice over time. However, maximal scotopic a- and b-wave amplitudes of HFD mice are decreased after 2 months and further decreased after 5 months of the diet regimen. Treatments with metformin for 3 months (HFD + Met) did not reverse the a- and b-wave amplitudes to the control level. $^{*,\#,\&}p < 0.05$.

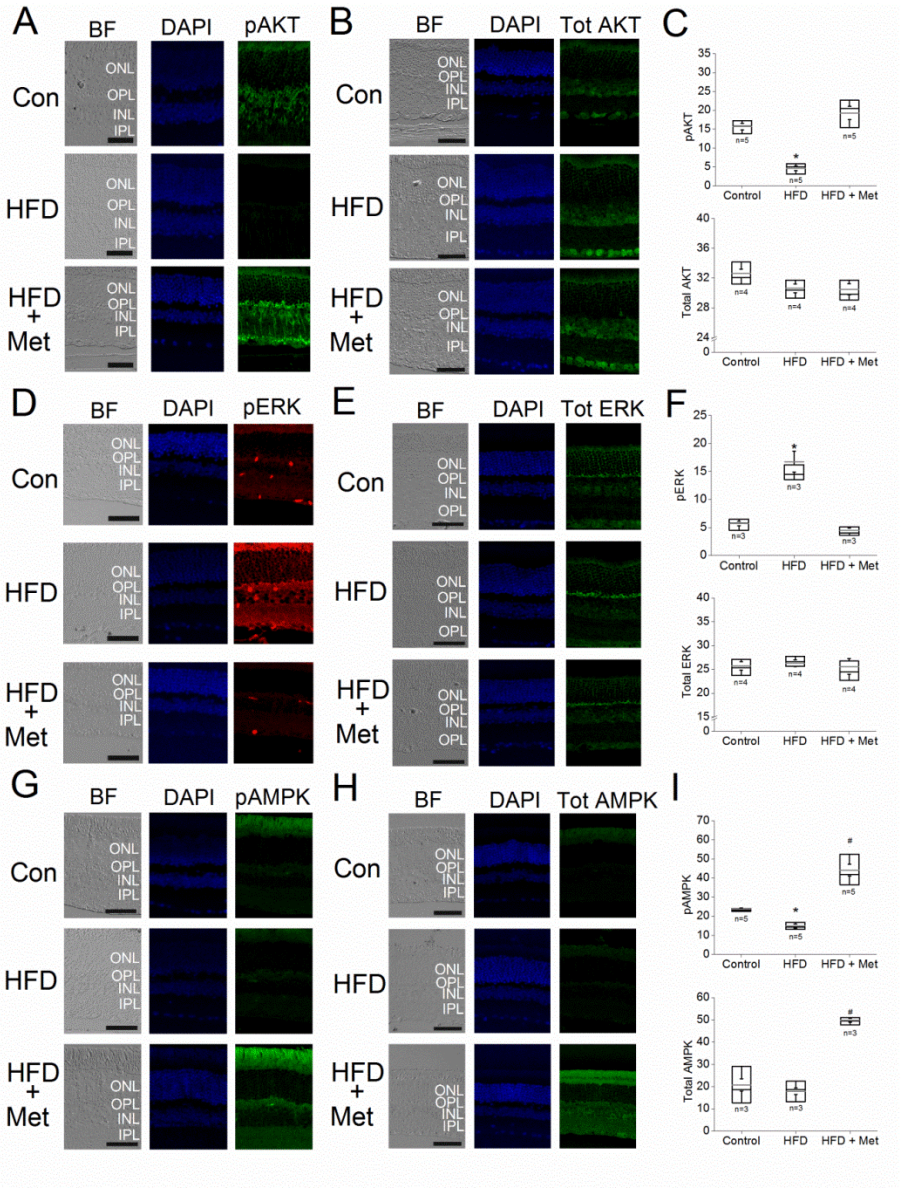

Figure 5. Metformin reverses HFD-induced effects on the immunofluorescent intensities of several proteins in mice retina. Mouse retinal sections (4 µm) were processed for immunofluorescent staining. Control mice (Con) were given standard chow for 7 months. The HFD mice (HFD) were given a HFD for 7 months. The HFD + metformin (HFD + Met) mice were given HFD for 7 months and treated with metformin for the last 5 months. (A-C) The fluorescent images of pAKT (A) and total AKT (B), and the statistical analyses of the fluorescent intensities in the control, HFD, and the HFD+Met retinas (C) are shown. The pAKT fluorescent intensity of HFD-retinas is significantly lower (*) than the other two groups. (D-F) The fluorescent images of pERK (D) and total ERK (E), and the statistical analyses of the fluorescent intensities in the control, HFD, and the HFD+Met retinas (F) are shown. The fluorescent intensity of pERK in the HFD mouse retina is significantly higher (*) compared to the control and the HFD+Met retinas. (G-I) The fluorescent images of pAMPK (G) and total AMPK (H), and the statistical analyses of the fluorescent intensities in the control, HFD, and the HFD+Met retinas (I) are shown. The fluorescent intensity of pAMPK in the HFD-retinas is significantly lower (*) compared to the control and HFD+Met retinas (*), while pAMPK is significantly higher in the HFD+Met mouse retina (#) compared to that of the control and HFD-retinas. The fluorescent intensity of total AMPK is significantly higher in the HFD+Met retina (#) compared to the other two groups. Scale bar = 50 µm. ONL, outer nuclear layer; OPL, outer plexiform layer; INL, inner nuclear layer; IPL, inner plexiform layer. (C, F, and I) The box-plots represent the distribution of fluorescent intensities within the specific group. The black line represents the median, and the gray line represents the mean of the specific group. N is the animal number of the group. $^{*,\#}p < 0.05$.

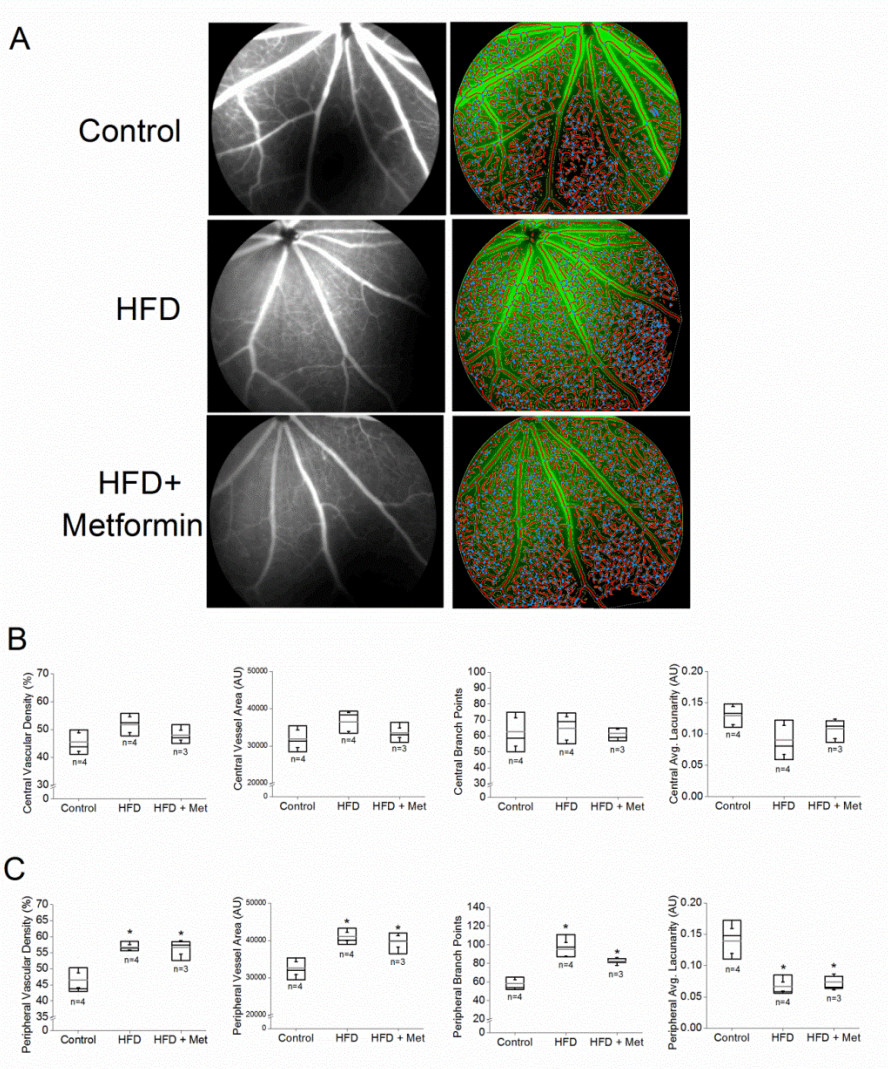

Figure 6. Metformin does not reverse HFD-induced neovascularization. Fluorescein angiography was used to determine the retinal vasculature in mice fed with normal chow (control), HFD for 6 months (HFD), or HFD mice treated with metformin (HFD+metformin). (A) The AngioTool software was used to determine the vascular parameters including vascular density, vessel area, the number of vessel branch points, and the average non-vascular space (avg. lacunarity). (B) There is no statistical difference in vascular density, vessel area, the number of branch points, and avg. lacunarity between control, HFD, and HFD + metformin (HFD+Met) mice in the central region of retinas. (C) In the peripheral regions of retinas, HFD-mice (HFD) and HFD-mice treated with metformin (HFD+Met) have statistical differences compared to the control (*) in vascular density, vessel area, number of branch points, and avg. lacunarity. The box-plots represent the distribution of fluorescent intensities within the specific group. The black line represents the median, and the gray line represents the mean of the specific group. N is the animal number of the group. $*, {}^{\#}p < 0.05$.

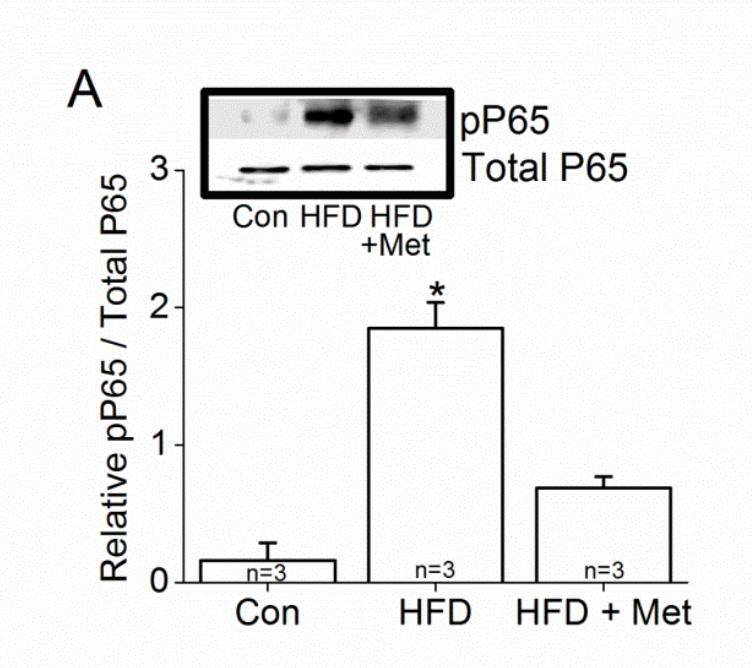

Figure 7. Metformin reduces HFD-induced inflammation. Retinas were collected from mice fed normal chow, HFD for 6 months, and HFD mice treated with metformin for the last 4 months. (A) Tissues were harvested and subjected to Western blot analysis of phosphorylated P65 (pP65) and P65 (Total P65; loading control). The HFD-retina has a significantly higher pP65 (*) compared to the other two groups.

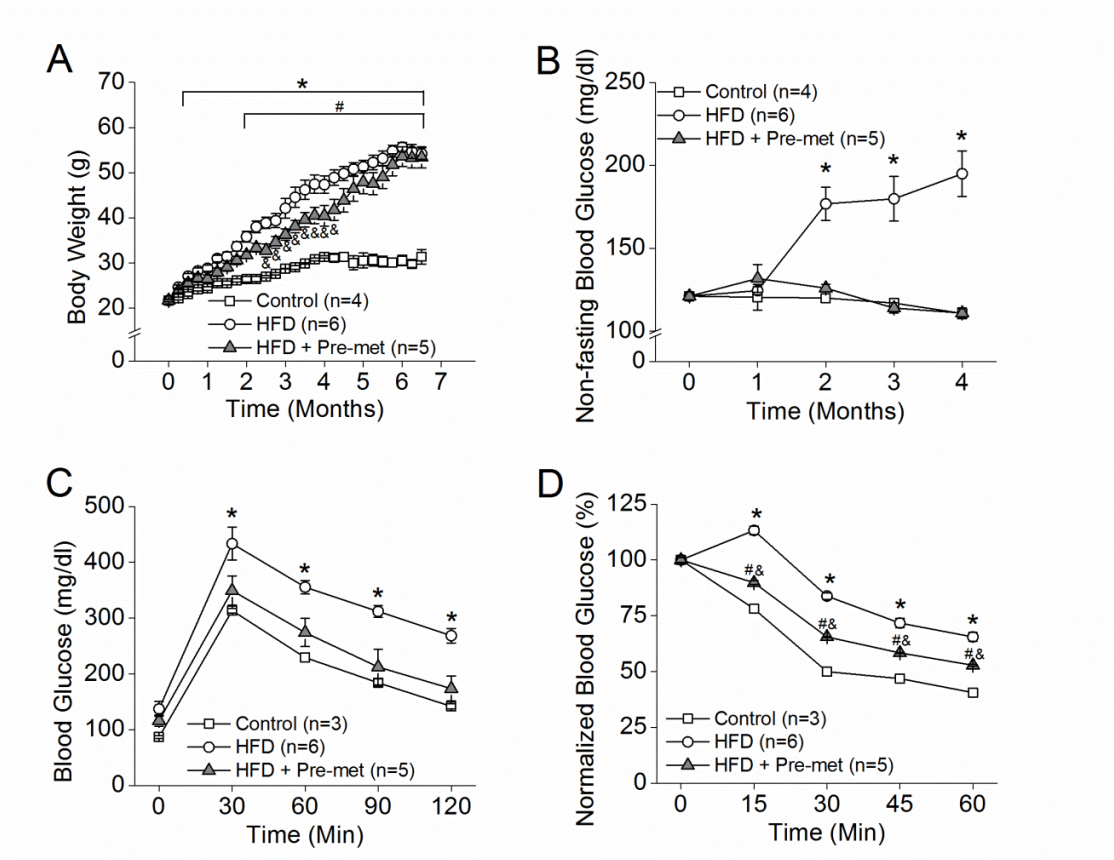

Figure 8. Metformin treatment delays body weight gain and prevent development of hyperglycemia in HFD-mice. Mice were fed a normal diet (Control), HFD, or a HFD with daily oral metformin treatment simultaneously (HFD + Pre-met). (A) Mice fed HFD had significant weight gain starting two weeks after HFD compared to the control (*). Mice fed a HFD and treated with metformin (HFD + Pre-met) did not have a significant weight gain until 9 weeks of HFD-feeding compared to the control (#). HFD mice treated with metformin (HFD + Pre-met) do not gain as much body weight as the HFD mice from weeks 11-19 (&). (B) HFD-fed mice had an increase of fasting blood glucose levels after 2 months of the diet regimen (*). However, HFD-fed mice treated with metformin do not develop hyperglycemia. (C) Treatment with metformin simultaneously with HFD-regimen from the beginning(HFD + Pre-met) prevents the development of glucose intolerance after 3 months of HFD. (D) HFD mice treated with metformin concurrently (HFD + Pre-met) show significant differences in insulin resistance compared to HFD-mice (&). $^{*,\#,\&}P < 0.05$.

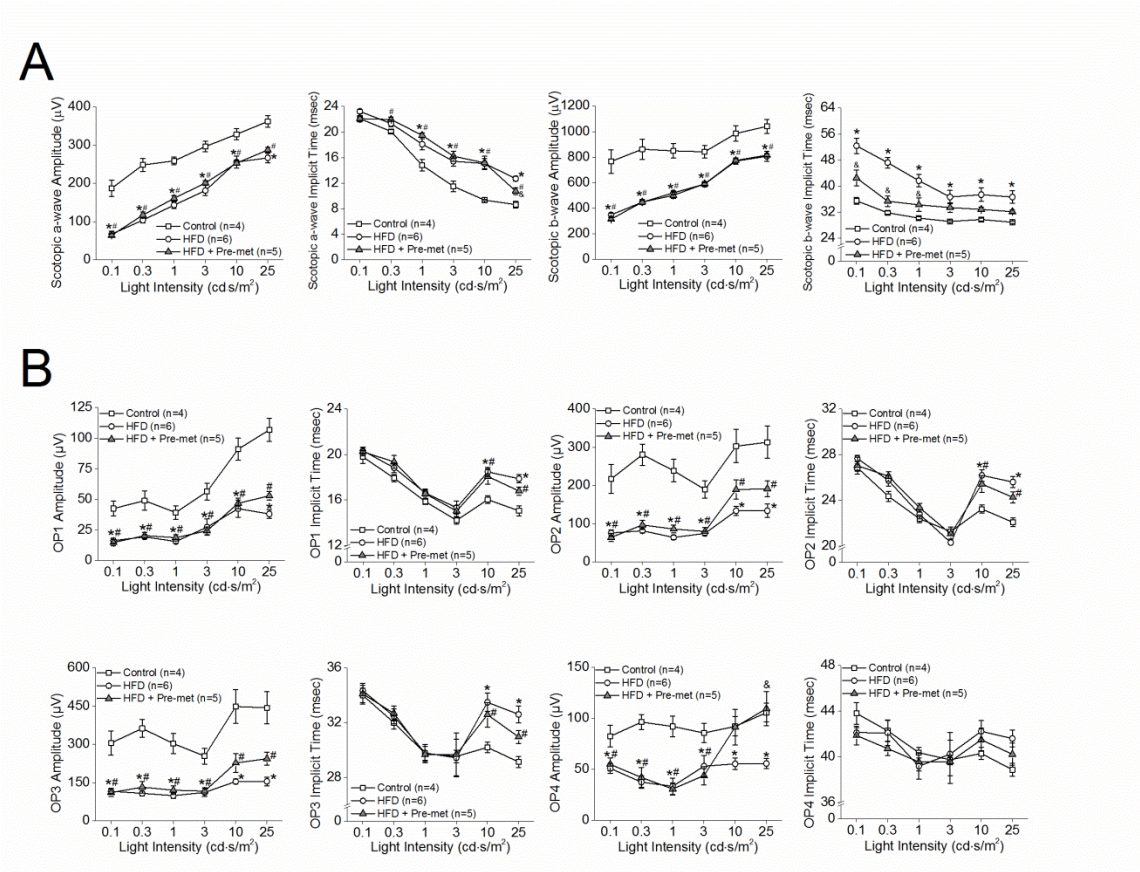

Figure 9. Concurrent metformin treatment does not prevent HFD-induced retinal dysfunction. Mice were fed a standard chow for 3 months (control), a HFD for 3 months (HFD), or a HFD with daily metformin treatments for 3 months (HFD+Pre-met). (A) HFD mice have decreased a- and b-wave amplitudes and delayed a- and b-wave implicit times compared to control mice (*). The HFD+Pre-met mice also have delayed a- and b-wave amplitudes and delayed a-wave implicit times compared to the control (#). However, HFD+Pre-met mice have improved b-wave implicit times compared to HFD mice (&). (B) The oscillatory potentials amplitudes were decreased and implicit times delayed in HFD- mice compared to controls (*) and also with HFD+Pre-met mice compared to controls (#). $^{*, \#, \&}P < 0.05$.

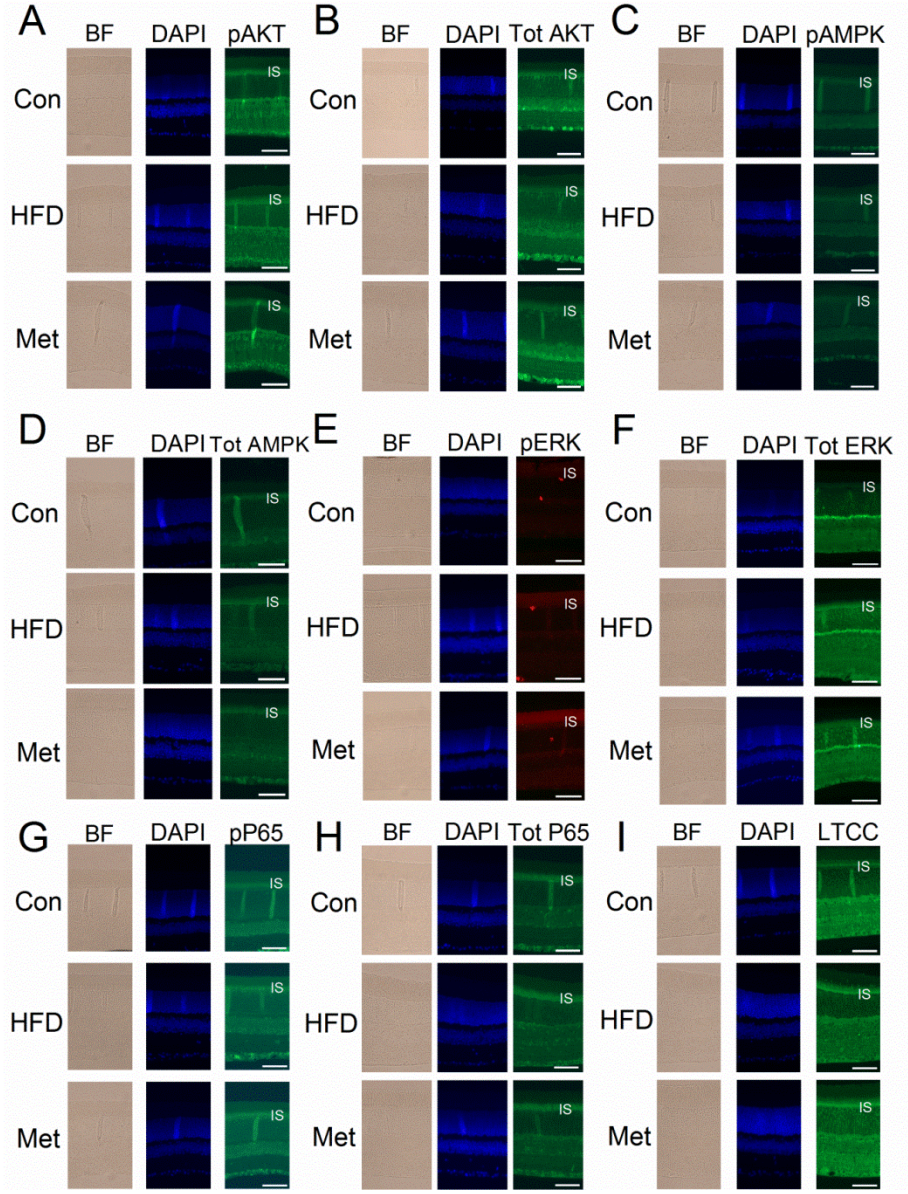

Figure 10. Metformin treatment for 1 month does not prevent HFD-induced changes in cell signaling in the retina. Each slide contained tissue from a mouse fed standard chow for 1 month (Con), a HFD for 1 month (HFD), and a HFD with daily metformin treatment simultaneously for 1 month (Met). The fluorescent images of pAKT (A), Total AKT (B), pAMPK (C), Total AMPK (D), pERK (E), Total ERK (F), pP65 (G), Total P65 (H) and L-type calcium channel Cav1.3 (I, LTCC) are shown. *Scale bar:* 50 µm. IS: inner segment.

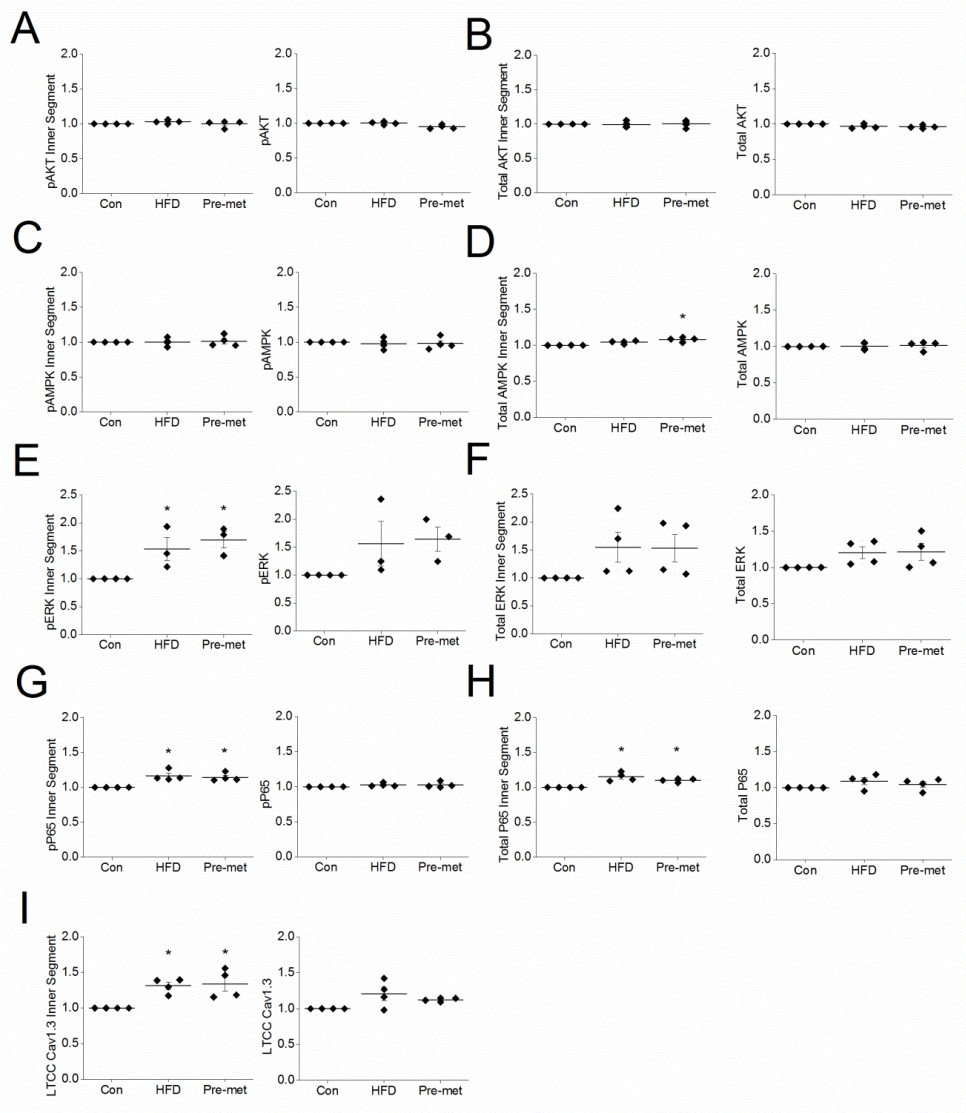

Figure 11. Quantification of immunofluorescent intensities of mouse retinal proteins after 1 month of feeding regimen. Each image in Figure 10 was quantified. The left panels represent quantifications of the inner segments of the photoreceptors, and the right panels represent quantifications across all the retinal layers (from the outer segments of photoreceptors to the ganglion cell layer). (A) pAKT; (B) Total AKT; (C) pAMPK; (D) Total AMPK; HFD mice treated with metformin (HFD+Pre-met) have increased Total AMPK fluorescent intensities in the inner segment compared to the control. (E) pERK; both HFD and HFD mice treated with metformin (HFD+Pre-met) groups have increased pERK fluorescent intensities in the inner segment compared to the control. (F) Total ERK; (G) pP65; both HFD and HFD+Pre-met groups have increased pP65 fluorescent intensities in the inner segment compared to the control. (H) Total P65; both HFD and HFD+Pre-met groups have increased Total P65 fluorescent intensities in the inner segment compared to the control. (I) LTCC Cav1.3; both HFD and HFD+Pre-met have increased LTCC Cav1.3 fluorescent intensities in the inner segment compared to the control. $^{*}P < 0.05$.